

Original Article

## A Model of Time-dependent Biodistribution of $^{153}\text{Sm}$ -Maltolate Complex and Free $^{153}\text{Sm}$ Cation Using Compartmental Analysis

Amir Hakimi<sup>1\*</sup>, Amir Reza Jalilian<sup>2</sup>, Ali Ghanbarzadeh<sup>3</sup>, Hamed Rezaee Jam<sup>4</sup>

### Abstract

#### Introduction

Compartmental analysis allows the mathematical separation of tissues and organs to determine activity concentration in each point of interest. Biodistribution studies on humans are costly and complicated, whereas such assessments can be easily performed on rodents.

In this study, we aimed to develop a pharmacokinetic model of  $^{153}\text{Sm}$ -maltolate complex as a novel therapeutic agent and free  $^{153}\text{Sm}$  cation in normal rats using compartmental analysis to evaluate the behavior of this complex.

#### Materials and Methods

We developed a physiologically-based pharmacokinetic model for scaling up the activity concentration in each organ with respect to time. In the mathematical model, physiological parameters including organ volume, blood flow rate, and vascular permeability were used. The compartments (organs) were connected anatomically, which allowed the use of scale-up techniques to predict new complex distribution in each body organ.

#### Results

The concentration of  $^{153}\text{Sm}$ -maltolate complex and free  $^{153}\text{Sm}$  cation in various organs was measured at different time intervals. The time-dependent behavior of the biodistribution of these two radiotracers was modeled, using compartmental analysis; the detected behaviors were drawn as a function of time.

#### Conclusion

The variation in radiopharmaceutical concentration in organs of interest could be described by summing seven to nine exponential terms, which approximated the experimental data with a precision of  $> 1\%$  in comparison with the original data from animal studies.

**Keywords:** Biodistribution, Modeling, Compartmental Analysis, Samarium- 153, Maltolate

---

1- Health Physics and Dosimetry Laboratory, Department of Energy Engineering and Physics, Amir Kabir University of Technology, Tehran, Iran

2- Nuclear Science Research School, Nuclear Science and Technology Research Institute, Tehran, Iran

3- Department of Medical Radiation Engineering, Science and Research Branch, Islamic Azad University, Tehran, Iran

4- Department of Medical Physics and Biomedical Engineering, Faculty of Medicine, Tehran University of Medical Sciences, Tehran, Iran

\*Corresponding author: +989123430288, E-mail: amir.hakimi@aut.ac.ir

## 1. Introduction

According to the principles of experimental techniques in human studies, use of data from the literature is one of the main recommended methods, which allows the realization of Reduce, Reuse and Recycling (3Rs) concept to decrease the number of required experimental procedures on animals and improve the outcomes [1].

Similarly, compartmental analysis supports the design of radiopharmaceuticals and permits the mathematical separation of tissues and organs to determine activity concentration in each point of interest and identify inconsistency in biodistribution and dosimetric studies. Additionally, by compartmental analysis, it is possible to consider different chemical species and predict the metabolites [2].

Mathematical models describing the kinetic process of a particular agent may be used to predict its behavior in regions where direct measurements are impossible, despite the availability of sufficient information on the physiology of the region for specifying its interrelationship with regions or tissues in which uptake and retention can be directly measured; these models can in fact account for the presence of metabolic products [3-6].

Compartmental modeling is the most commonly applied method for describing the uptake and clearance of radioactive tracers in tissues [7-9]. These models specify that all tracer molecules, delivered or injected to the system, exist in one of many compartments at any given time. Each compartment defines one possible state of the tracer, specifically its physical location (e.g., intravascular, extracellular, and intracellular spaces and synapse) and chemical state (e.g., the current metabolic form or its binding to different tissue elements such as plasma proteins and receptors). Often, a single compartment represents a number of these states combined together; compartments are typically numbered for mathematical information [10]. The compartmental model also describes the possible transformations which can happen to the tracer, thus allowing its movement

between compartments. This model defines a fraction or proportion of tracer molecules, moving to a different compartment within a specific time frame. The fractional rate of change in the tracer concentration in one compartment is known as a rate constant and contains units of inverse time [10].

The physiological interpretation of the source and destination compartments defines the implication of rate constants for tracer movement between the compartments. For an inert, freely diffusible tracer, the rate constant of transfer from arterial blood to the tissue compartment defines the local blood flow. Through determining these rate constants (or some algebraic combinations), quantitative estimates or indices of local physiological parameters can be obtained.

Overall, the underlying goal of all modeling methods is to estimate one or more of these rate constants from tissue radioactivity measurements [2, 10]. In this study, compartmental analyses were performed to generate a time-dependent model of the biodistribution of somarium-153 [<sup>153</sup>Sm]-maltolate complex as an efficient and novel therapeutic agent and free <sup>153</sup>Sm cation in order to overcome possible lymphatic malignancies [11, 12].

Maltol (3-hydroxy-2-methyl-4-pyrone), a common product formed upon heating of carbohydrates, is an approved food additive used to impart desirable malty flavors and odor to bread, cakes, beer, and other beverages (Figure 1). Maltol loses its hydroxyl proton at neutral to basic pH levels, forming a maltolate anion. This anionic molecule forms a strong bidentate/tridentate chelating agent with gallium, iron, zinc, aluminum, vanadium [13], and lanthanides [14].

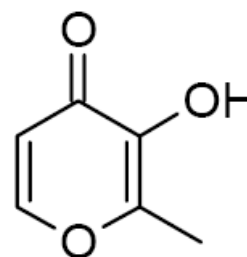


Figure 1. The chemical structure of maltolate

Most maltolate metal complexes are reported as biologically active compounds. Gallium maltolate is a superior oral anti-tumor agent in clinical trials, unlike gallium nitrate and various metal-based anti-tumoral compounds. Ga-maltolate is an effective anti-lymphatic compound showing activity against Ga nitrate-resistant lymphomas [15] and urothelial malignancies [16].

Tris(maltolato) gallium (III) complex has been used in the treatment of several lymphoma cell lines, including those resistant to Ga-nitrate [17]. Considering the interesting pharmacological properties of maltolato complexes such as solubility in serum, rapid washout, tumor avidity, and feasible complexation with various metals, *tris* (maltolato) Ga-67 (III) was developed as a possible tumor imaging agent in single-photon emission computed tomography (SPECT) [18].

In the literature, owing to the success of oral Ga-maltolate preparations and importance of palliative therapies for bone pain in various metastatic carcinomas,  $^{177}\text{Lu}$ -maltolate ( $^{177}\text{Lu}$ -Mal) has been used as a potential therapeutic complex for determining bone uptake around the world [18]. Besides the application of maltolate radioactive compounds in diagnosis and treatment of malignancies,  $^{153}\text{Sm}$ -maltolate was developed to evaluate the safety of maltol as a detoxifying agent in metal compounds [11, 12].

Mathematical biodistribution models constitute an alternative approach to direct calculation of cumulated activity in field of radiopharmaceutical dosimetry. It is often impractical to measure the time-activity curves of all source regions. However, when physiological interactions of these regions with blood or other directly measurable tissues are identified, the time-activity curves of unmeasured tissues can be inferred by these models. Biodistribution modeling can be also used to separate activities in regions which overlap on imaging studies, such as renal cortex, renal pelvis, liver, and right colon [6]. In future, biodistribution modeling will play an

important role in molecular imaging and in-vivo dosimetry.

Development of lanthanide mobilization protocols using non-toxic, human-approved chelators is an interesting field in human health studies [11]. In the present research, we developed a time-dependent model based on the biodistribution of  $^{153}\text{Sm}$ -maltolate complex, using compartmental analysis and compared the findings with free  $^{153}\text{Sm}$  cation.

## 2. Materials and Methods

### 2.1. Preparation of $^{153}\text{Sm}$ -Mal

Samarium-153 was produced by neutron irradiation of 1 mg of enriched [ $^{152}\text{Sm}$ ] $\text{Sm}_2\text{O}_3$  ( $^{152}\text{Sm}$ , 98.7%, ISOTECH Inc. (Miamisburg, OH, USA)) according to the reported procedures [19] at a thermal neutron flux of  $5 \times 10^{13} \text{ n.cm}^{-2}.\text{s}^{-1}$  for five days in Tehran Research Reactor.

Although most conducted studies have reported the synthesis of maltolate metal complex in the aqueous phase [1], in the present study, synthesis was performed in ethanolic media. Briefly,  $^{153}\text{SmCl}_3$  (3 mCi, 0.1 ml) was added to a borosilicate vial and dried by heating ( $50^\circ\text{C}$ ) under a nitrogen flow for nearly 15 min. Then, maltol (30 mg, 0.25 mmol) was dissolved in absolute ethanol (1 ml) and added to the dried residue; the mixture was agitated and incubated at  $60^\circ\text{C}$  for 2 h. After obtaining the desired radiochemical purity, the ethanolic solution was concentrated to 0.05 ml by warming at  $40\text{--}50^\circ\text{C}$ ; the solution was then diluted to a 5% solution by adding 1 ml of normal saline.

### 2.2. Biodistribution of [ $^{153}\text{Sm}$ ]-maltolate and $^{153}\text{SmCl}_3$ in normal rats

To determine the comparative biodistribution, [ $^{153}\text{Sm}$ ]-maltolate and  $^{153}\text{SmCl}_3$  were administered to normal rats in separate groups ( $n=3$  per group). Then, 100–120  $\mu\text{l}$  of the final  $^{153}\text{Sm}$ -maltolate solution ( $4800 \pm 185 \text{ kBq}$ ) was intravenously injected to rats through the tail vein. The animals were sacrificed at specific time intervals (2, 4, 24, and 48 h). The specific activity of different organs was calculated as the percentage of injected dose per gram, using a high-purity germanium (HPGe) detector.

### 2.3. Modeling of <sup>153</sup>Sm-maltolate and <sup>153</sup>Sm-free cation

The first approach of biodistribution modeling in this study included the knowledge of chemical kinetics, mimetism of samarium, and the possible targets of diagnosis/therapy to select the possible models for replacing standard sampling methods in experimental studies [20, 21]. A model with only one physical compartment (whole body) and one chemical compartment, i.e., <sup>153</sup>Sm-maltolate, was generated, using compartmental analysis. The values used in this study included the residence times from three different studies performed on free <sup>153</sup>Sm cation(whole body, average excretion, and maximum excretion as the chemical compartment) and the activity concentration values (as a function of time) in whole body and in blood samples . More consistence could be obtained considering the two sources of data in one single modeling. The next step was the statistical analysis of biodistribution and dosimetry in rats with

respect to three chemical fractions of the designed radiopharmaceutical: [<sup>153</sup>Sm]-maltolate, free <sup>153</sup>Sm cation, and total radiopharmaceutical (free <sup>153</sup>Sm+<sup>153</sup>Sm-Mal) (Figure 2). By applying mammillary models with six compartments and human anatomical data from the International Commission on Radiological Protection (ICRP) Publication 89, studies were also performed on rats. The selected parameters were highly critical, considering the blood flux in each body region and tissue.

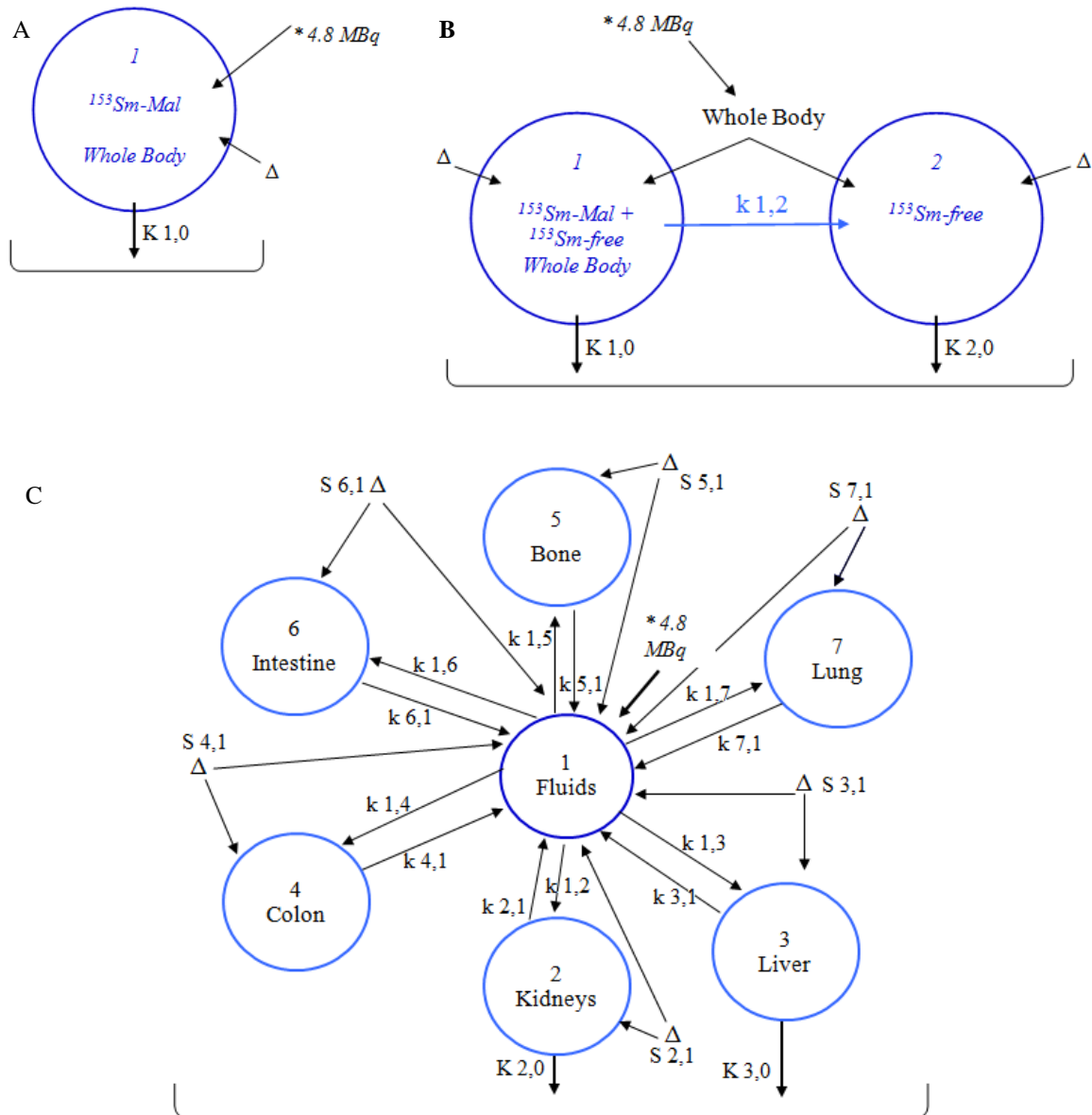
## 3. Results

### 3.1. Time-dependent model of <sup>153</sup>Sm-maltolate

The activity concentration in each organ was measured by the use of detectors at specific time intervals after injection; the results show variation with time. The compartmental model was used to present a mathematical description of these variations. The equations presented in table 1 were obtained for each organ. In each case,  $t=0$  corresponds to the time of injection (Figure 3):

Table 1: Time-dependent model of <sup>153</sup>Sm-maltolate in normal rats

No.	Organ	Time-dependent model
1	Blood	$f_1 = 1.594026 e^{-0.45t} + (3.78E-1) e^{-0.077t} + (9.45E-2) e^{-(9.9E-4)t} + (4.116E-4) e^{-0.001t} + (7.224E-5) e^{-0.06t} - (5.964E-8) e^{-0.14t} - (3.885E-5) e^{-5.04t}$
2	Heart	$f_2 = (1.0433E4) e^{5.04t} + (8.745E-1) e^{-1.64t} + (1.1055E-2) e^{-0.14t} + (9.72E-3) e^{-0.006t} + (7.2E-2) e^{0.019t} + (8.4E-2) e^{-0.091t}$
3	Bone	$f_3 = (9.06134E-1) e^{(9.9E-4)t} + (2.174354E-5) e^{-1.6t} - (4.7715399E-1) e^{-0.47t} - (1.793888E-1) e^{-1.64t} - (2.835115E-1) e^{-0.14t} - (5.2383E-2) e^{0.057t} - (1.51635E-2) e^{-0.0025t}$
4	Colon	$f_4 = (1.18E-2) e^{(9.9E-4)t} + (1.1564E-2) e^{-0.001t} + (2.0296E-2) e^{-0.06t} + (1.652E-1) e^{-0.087t} - (3.413378035E-1) e^{-0.62t} - (1.0915E-2) e^{-0.973t} (1.6756E-2) e^{-0.14t} - (3.413378035E-1) e^{-1.00t}$
5	Intestine	$f_5 = (9.9456E-2) e^{-0.061t} + (1.48E-2) e^{-(9.9E-4)t} + (2.072E-1) e^{-0.079t} - (5.8118601E-2) e^{-0.57t} - (9.509E-3) e^{-1.953t} - (7.4E-5) e^{-0.15t} (1.4504E-2) e^{-0.001t} - (4.281159E-1) e^{-1.18t}$
6	Kidney	$f_6 = (7.5143E-1) e^{(9.9E-4)t} + (3.688E-1) e^{-0.77t} - (1.58584E-4) e^{-0.06t} - (8.5285E-2) e^{-5.04t} - (1.30924E-2) e^{-0.14t} - (9.0356E-5) e^{-0.001t} (9.22E-4) e^{0.1t}$
7	Liver	$f_7 = 9.09696 e^{-1.561t} + (3.09E-3) e^{-1.15t} + (5.7165E-1) e^{-0.099t} + (1.545E-1) e^{-0.001t} + 8.652 e^{-0.0461t} - 2.426844285 e^{-0.18t} - (1.80765E-1) e^{-0.913t} - (1.7876844285E1) e^{-0.9498t}$
8	Lung	$f_8 = (6.44E-1) e^{-0.079t} + (7.912E-2) e^{-0.061t} + (4.6E-2) e^{-(9.9E-4)t} + (4.508E-2) e^{-0.001t} - (1.80638895E-1) e^{-0.57t} - (6.555E-3) e^{-0.953t} - (2.3E-4) e^{-0.15t} - 1.330638895 e^{-1.018t}$
9	Spleen	$f_9 = 1.892134 e^{(9.9E-4)t} + (4.540354E-5) e^{-0.6t} - 1.95586399 e^{-0.44t} - (3.745888E-3) e^{-1.64t} - (4.001115E-4) e^{-0.14t} - (1.09383E-1) e^{-0.057t} - (3.16635E-2) e^{-0.0025t}$
10	Sternum	$f_{10} = (2.3933E-1) e^{-0.199t} + (1.7836E-1) e^{-0.01t} + (4.004-2) e^{-1.6t} + (4.550637E-2) e^{0.0523t} - (8.364811E-1) e^{-0.84t} - (1.6835E-2) e^{-0.04t} - (4.4044E-2) e^{-0.14t} - (3.913E-4) e^{0.107t}$
11	Stomach	$f_{11} = (1.82E-2) e^{-(9.9E-4)t} + (3.1304E-2) e^{-0.06t} + (2.548E-1) e^{-0.077t} + (5.63836E-3) e^{-0.01t} - (2.5844E-2) e^{-0.14t} - (5.264701715E-1) e^{-0.63t} (1.6835E-2) e^{-0.973t} - 1.436462 e^{-2.17t}$



\*→ 4.8 MBq intravenous injection of  $^{153}\text{Sm}$  in the blood (time=0),  
 $\Delta$ : Sampling for biokinetic calculations,  
 $K_{i,0}$ : Removal constant from organs  
 $k_{i,j}$ : Transfer constant from blood to tissues and organs,  
 $k_{i,j}$ : Transfer constant from tissues and organs to body fluids.

Figure 2. Scheme of the selected compartmental analysis model. A) one physical compartment (whole body) and one chemical compartment ( $^{153}\text{Sm-Mal}$ ), B) one physical compartment (whole body) and two chemical compartments ( $^{153}\text{Sm-Mal}$  and free  $^{153}\text{Sm}$ ), C) six-compartmental model for rats

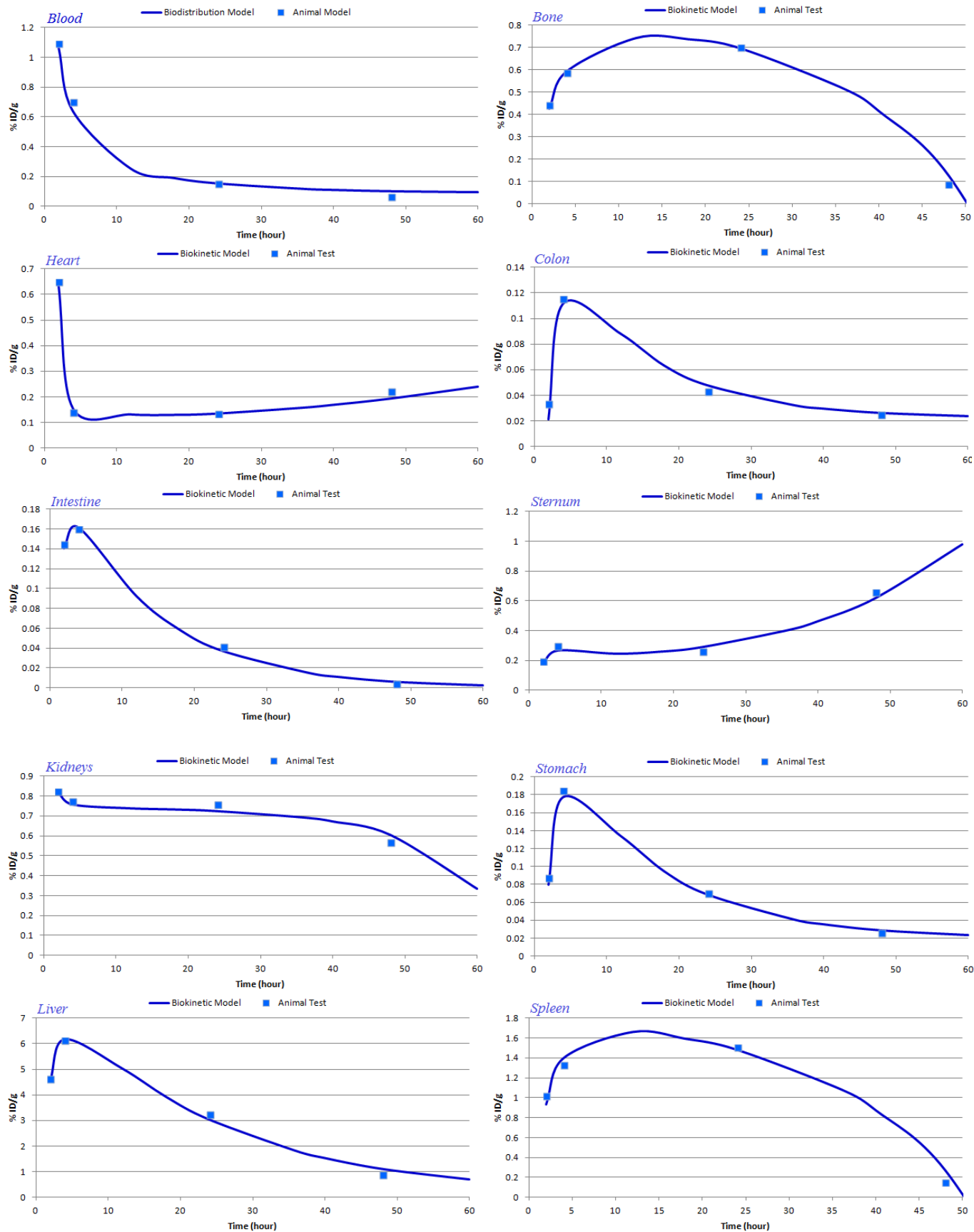


Figure 3. The temporal behavior of <sup>153</sup>Sm-Mal biodistribution in various organs of wild-type rats.

The deviation of <sup>153</sup>Sm-Mal concentration in all organs and tissues is described by summing seven to nine exponential terms. The comparison between the model and data from animal studies showed a precision of > 1% in biodistribution models. It should be noted that the activity concentration was in an acceptable statistical range.

**3.2. Time-dependent model of free <sup>153</sup>Sm cation**  
 The distribution of free <sup>153</sup>Sm cation was measured by the use of detectors at particular time intervals after injection in each organ. Similar to the previous step, the compartmental model was used to present a mathematical description of variations in biodistribution of free <sup>153</sup>Sm cation. The consecutive equations (table 2) were obtained for each organ. In each case, t=0 corresponds to the time of injection:

Table 2: Time-dependent model of free <sup>153</sup>Sm in normal rats

No.	Organ	Time-dependent model
1	Blood	$f_1 = (1.497582E-1) e^{(9.9E-4)t} + (3.262714E-6) e^{-0.6t} + (2.27535E-3) e^{0.0025t} - (2.09499059E-1) e^{-0.001t} - (2.691808E-3) e^{-1.64t} - (2.875215E-2) e^{-0.14t} - (3.1717E-4) e^{0.051t} - (1.36521E-3) e^{0.057t}$
2	Heart	$f_2 = (1.59012E-1) e^{(9.9E-4)t} + (8.68256E-2) e^{-0.06t} + (4.94704E-4) e^{-0.001t} + (4.2908E-1) e^{-0.97t} - (2.99094E-1) e^{-1.29t} - (1.474016E-3) e^{-0.135t} - (4.71988E-3) e^{0.057t}$
3	Bone	$f_3 = 1.15893 e^{(9.9E-4)t} + (5.688E-1) e^{-0.967t} - (1.31535E-1) e^{-9.14t} - (2.01924E-1) e^{-1.13t} - (6.6834E-2) e^{-0.06t} - (1.3509E-3) e^{-0.00112t} - (2.9862E-3) e^{0.0911t}$
4	Intestine	$f_4 = (6.678E-2) e^{(9.9E-4)t} + (3.6464E-2) e^{-0.06t} + (2.0776E-4) e^{-0.001t} + (8.162E-4) e^{0.0047t} + (1.802E-1) e^{-0.97t} - (2.1041E-1) e^{-1.08t} - (6.1904E-4) e^{-1.735t}$
5	Kidney	$f_5 = 1.51753 e^{(9.9E-4)t} + (7.448E-1) e^{-0.977t} - (1.72235E-1) e^{-9.04t} - (2.64404E-1) e^{-1.14t} - (3.20264E-1) e^{-0.06t} - (1.82476E-4) e^{-0.001t} - (1.862E-3) e^{0.09t}$
6	Liver	$f_6 = 2.73168 e^{(9.9E-4)t} + 1.491584 e^{-0.063t} + 7.3712 e^{-0.967t} + (8.4985E-3) e^{-0.00103t} + (3.33872E-2) e^{0.04764t} - 8.60696 e^{-1.0812t} - (2.532224E-2) e^{-1.645t}$
7	Lung	$f_7 = (4.564E-1) e^{(9.9E-4)t} + (2.24E-1) e^{-0.967t} + (3.388E-1) e^{-0.154t} - (3.5952E-1) e^{-1.13t} - (2.632E-1) e^{-0.06t} - (2.2288E-1) e^{-0.00112t} - (1.176E-3) e^{0.094t}$
8	Spleen	$f_8 = 1.2714 e^{(9.9E-4)t} + (6.24E-1) e^{-0.6t} - (9.438E-1) e^{-0.147t} - 1.00152 e^{-1.12t} - (7.332E-1) e^{-0.0624t} - (6.2088E-1) e^{-0.00102t} - (3.276E-3) e^{0.097t}$
9	Stomach	$f_9 = (6.4E-3) e^{(9.9E-4)t} + (1.98272E-3) e^{-0.001t} + (2.49088E-1) e^{-0.14t} + (5.92E-3) e^{-0.973t} + (1.1008E-3) e^{-0.062t} + (8.64E-2) e^{-0.077t} + (1.216E-2) e^{0.0523t} - (1.85132368E-1) e^{-0.43t} - (2.51296E-3) e^{-0.017t} - (2.171312E-1) e^{-1.18t}$

**4. Discussion**

Regarding the blood activity, the <sup>153</sup>Sm cation content remained almost intact within 48 h, which can be a result of metal-serum protein interactions, while for <sup>153</sup>Sm-Mal, the activity rapidly diminished in 24 h and reached the minimum level within 48 h. With regard to the kidney activity, both compounds were excreted from the kidneys, although the difference was not significant.

Generally, the bone activity is always a major problem in lanthanide overdose. The <sup>153</sup>Sm cation content was almost higher at all time intervals, compared to the labeled compound; also, in 48 hours, almost no activity (< 0.4%) could be observed in the bones. The liver activity content is another major problem in lanthanide overdose. The <sup>153</sup>Sm cation content

was almost lower in the first few hours, while it remained constant at nearly 3% after 24 h. The whole liver activity decreased to less than 2% within 48 h, which is a satisfactory level of reduction in the detoxification process.

**5. Conclusion**

In this study, time-dependent biodistribution model of <sup>153</sup>Sm-Mal and free <sup>153</sup>Sm cation was developed by using compartmental analysis with respect to anatomic data from ICRP Publication 89. Biodistribution studies of free <sup>153</sup>Sm cation and <sup>153</sup>Sm-Mal were carried out in wild-type rats in comparison with the uptake of critical organs. Comparative studies on Sm<sup>3+</sup> cation and the labeled compound were conducted for 48 h, demonstrating a more rapid washout activity for the labeled

compound. An effective half-life of nearly 2.3 h was calculated for the complex with a biological half-life of 2.46 h. Radioactivity in case of the labeled compound was significantly removed from the blood and bone. Through modeling, the variation of pharmaceutical concentration in all organs was described by summing seven to nine exponential terms, which approximated the experimental data with a precision of > 1%; however, further research is required to complement such models. The final goal of modeling is incorporating the activity of beta-emitting nuclides in order to determine toxicity and its effect on cellular apoptosis. A

stochastic approach can be adapted to model beta emission, since the distance a particle is emitted varies randomly over time. This theoretically improved model can be implemented for simulations involving dosimetric calculations.

### Acknowledgments

The sincere assistance provided by Dr. Shirvani- Arani and Dr. Bahrami- Samani is highly appreciated.

### References

1. Russell, W. M. S., R. L. Burch, et al. (1959). "The principles of humane experimental technique."
2. Sardari D , Hakimi A. Modeling the time dependent distribution of a new <sup>153</sup>Sm complex for targeted radiotherapy purpose. *Rep PractOncol Radiother.*2012; 19(3):214-20.
3. Foster DM , Boston RC. The use of computers in compartmental analysis: the SAAM and CONSAM programs. In *Compartmental distribution Radiotracers.* 1983:73–142.
4. Bogen DK. Simulation software for the Macintosh. *Science.* 1989 Oct;246:138-42.
5. Ralston, M. L. (1979). Fitting pharmacokinetic models with BMDPAR, BMDP Statistical Software, Department of Biomathematics, University of California, Los Angeles.
6. Siegel JA, Thomas SR, Stubbs JB, Stabin MG. MIRD pamphlet no. 16: techniques for quantitative radiopharmaceutical biodistribution data acquisition and analysis for use in human radiation dose estimates. *The Journal of Nuclear Medicine.* 1999 Feb 1;40(2):37S.
7. Jacquez JA. *Compartmental analysis in biology and medicine.* Ann Arbor: University of Michigan Press; 1985 Sep.
8. Anderson DH. Springer-Verlag; New York: 1983. *Compartmental modeling and tracer kinetics*; p. 302
9. Carson RE. Tracer kinetic modeling in PET. In: Bailey D.L., Townsend D.W., Valk P.E., Maisey M.N., editors. *Positron emission tomography: basic sciences.* 2nd ed. Springer; London, UK: 2005. pp. 127–59.
10. Townsend DW, Valk PE, Maisey MN. *Positron emission tomography.* Springer-Verlag London Limited; 2005.
11. Naseri Z, Hakimi A, Jalilian AR, Nemati Kharat A, Bahrami-Samani A, and Ghannadi-Maragheh M. Preparation and quality control of the [<sup>153</sup>Sm]-Samarium Maltolate complex as a lanthanide Mobilization product in rats. *Sci Pharm.*2011 jun; 79(2):265-75.
12. Rezaeejam H, Hakimi A, Jalilian AR, Abbasian P, Shirvani-Aran S, Ghannadi-Maragheh M. Determination of human absorbed dose from [<sup>153</sup>Sm]-Samarium maltolate based on distribution data in rats. *Int. J. Radiat. Res.* 2015 Apr ; 13(2):173-80.
13. Bernstein LR, Tanner T, Godfrey C, Noll B., *Chemistry and Pharmacokinetics of Gallium Maltolate, a compound with high oral Gallium Bioavailability.* *Met Based Drugs.* 2000; 7: 33–48.
14. Thompson KH, Barta CA, Orvig C., *Metal complexes of maltol and close analogues in medicinal inorganic chemistry.* *Chem Soc Rev.* 2006; 35: 545–56.
15. Chitambar CR, Purpi DP, Woodliff J, Yang M, Wereley JP. Development of gallium compounds for treatment of lymphoma: gallium maltolate, a novel hydroxypyrrone gallium compound, induces apoptosis and circumvents lymphoma cell resistance to gallium nitrate. *Journal of Pharmacology and Experimental Therapeutics.* 2007 Sep 1;322(3):1228-36.

16. Chitambar CR. Gallium nitrate for the treatment of non-Hodgkin's lymphoma. Expert opinion on investigational drugs. 2004 May 1;13(5):531-41.
17. Fazaeli Y, Jalilian AR, Mohammadpour Amini M, Majdabadi A, Rahiminejad A, Bolourinovin F, Pouladi M. Development of Ga-67 maltolate complex as an imaging agent. Iranian Journal of Pharmaceutical Research. 2012 May 20;11(3):755-62.
18. Hakimi A, Jalilian AR, Shirvani-Arani S, Abbasian P, Khoshmaram V, and Ghannadi-Maragheh M. Production, quality control, biological evaluation and biodistribution modeling of Lutetium-177 maltolate as a viable bone pain palliative in skeletal metastasis. Journal of Radioanalytical and Nuclear Chemistry 2015 Jan;303(1):1-10.
19. Iyer, S. R. and Knapp, F. F., Jr. Editors, for, "Manual for Reactor Production of Radioisotopes," International Atomic Energy Agency (IAEA), TECDOC-1340; Vienna, Austria, January 2003 (ISBN-92-0-101103-2).
20. Abbasian P, Foroghy M, Jalilian AR, Hakimi A, Shirvani-Arani S. Modeling the time dependent biodistribution of Samarium-153 ethylenediamine tetramethylene phosphonate using compartmental analysis. Reports of Practical Oncology & Radiotherapy. 2014 Jun 30;19(3):214-20.
21. Moghaddam AK, Hakimi A, Mardanshahi A, Jalilian AR, Amirfakhrian H, Anijdan HM. Compartmental Analysis to Predict the Biodistribution of [166Ho]-DOTA-Bevacizumab for Targeted Radiotherapy Purpose. Frontiers in Biomedical Technologies. 2015 Dec 9;2(3):118-27.